Short Communication

Structural and functional integrity of the coxsackievirus B3 *ori*R: spacing between coaxial RNA helices

Mark J. M. van Ooij,[1] Dirk H. R. F. Glaudemans,[1] Hans A. Heus,[2] Frank J. M. van Kuppeveld[1] and Willem J. G. Melchers[1]

[1]Radboud University Medical Centre Nijmegen, Nijmegen Centre for Molecular Life Sciences, Department of Medical Microbiology, PO Box 9101, 6500 HB Nijmegen, The Netherlands

[2]Radboud University Nijmegen, Institute for Molecules and Materials, Laboratory of Biophysical Chemistry, University of Nijmegen, Toernooiveld 1, 6525 ED Nijmegen, The Netherlands

Correspondence
Willem J. G. Melchers
w.melchers@ncmls.ru.nl

Received 26 September 2005
Accepted 19 November 2005

The enterovirus *ori*R is composed of two helices, X and Y, anchored by a kissing (K) interaction. For proper *ori*R function, certain areas of these helices should be specifically oriented towards each other. It was hypothesized that the single-stranded nucleotides bridging the coaxial helices (Y–X and K–Y linkers) are important to determine this orientation. Spatial changes were introduced by altering the linker length between the helices of the coxsackievirus B3 *ori*R. Changing the linker lengths resulted in defective RNA replication, probably because of an altered *ori*R geometry. The identity of the linker residues also played a role, possibly because of sequence-specific ligand recognition. Although each point mutation altering the primary sequence of the Y–X spacer resulted in defective growth at 36 °C, the mutations had a wild-type phenotype at 39 °C, indicating a cold-sensitive phenotype. The results show that the intrinsic connection between *ori*R structure and function is fine-tuned by the spacing between the coaxial RNA helices.

Replication of single-stranded viral RNA genomes of positive polarity, such as enteroviruses, is accomplished by RNA-dependent RNA polymerases (RdRps). Initiation of minus-strand synthesis demands positioning of the RdRp in close proximity to the 3′ end of a plus strand, whereas the RdRp should be placed at the 3′ end of a minus strand to initiate synthesis of a plus strand. As the 3′ ends of the complementary strands are dissimilar, the replication machinery recognizes two different types of *cis*-acting elements to initiate synthesis of (+) and (−) strands, *ori*L and *ori*R (Agol *et al.*, 1999).

The enterovirus *ori*L is involved in virus replication and translation (Andino *et al.*, 1990; Barton *et al.*, 2001; Gamarnik & Andino, 1998). This conserved element folds into a cloverleaf structure and interacts with diverse viral and host proteins (Andino *et al.*, 1990; Gamarnik & Andino, 2000; Harris *et al.*, 1994; Parsley *et al.*, 1997). The existence and functional importance of a ribonucleoprotein (RNP) complex, involving *ori*L interacting with the virus protein 3CD and the cellular factor PCBP, are required for genome circularization and RNA synthesis (Barton *et al.*, 2001; Herold & Andino, 2001).

The enterovirus *ori*R is involved in the initiation of (−)-strand RNA synthesis (Melchers *et al.*, 1997; Pilipenko *et al.*, 1996). We have shown that sequences within the loop of domain X base pair with complementary sequences in the loop of domain Y to form an intramolecular tertiary structural element, designated a 'kissing' interaction (K domain) (Fig. 1a). The functional significance of the K domain is evident, as mutations introduced to destabilize this structure resulted in inactivated viruses, severely impaired mutants or the accumulation of revertants with a restored kissing interaction (Mirmomeni *et al.*, 1997; Pilipenko *et al.*, 1996; Wang *et al.*, 1999). The K domain can be stacked onto the helix of domain X to form one coaxial helical domain that, connected to domain Y, determines the overall structure of the *ori*R (Melchers *et al.*, 1997; Pilipenko *et al.*, 1996). Thus, the enteroviral *ori*R can be viewed as two elongated helices (Fig. 1a–c). We previously found that the kissing structure is relatively stable and that it may serve as an anchor to orient the attached helical elements (Wang *et al.*, 1999). We suggested that the mutual orientation of the X and Y helices is critical to ensure a proper *ori*R function and that certain areas of these two helical domains should crosstalk (Melchers *et al.*, 2000). This crosstalk might be important for the simultaneous interaction with ligands, probably required to form an RNP composed of viral (Harris *et al.*, 1994) and host (Mellits *et al.*, 1998; Todd *et al.*, 1995; Waggoner & Sarnow, 1998) proteins. Here, we hypothesize that the single-stranded nucleotides bridging the coaxial helices (Y–X and K–Y linkers; Fig. 1a–c) are important to determine this spatial orientation.

A rotating version of Fig. 1(c) is available as supplementary material in JGV Online.

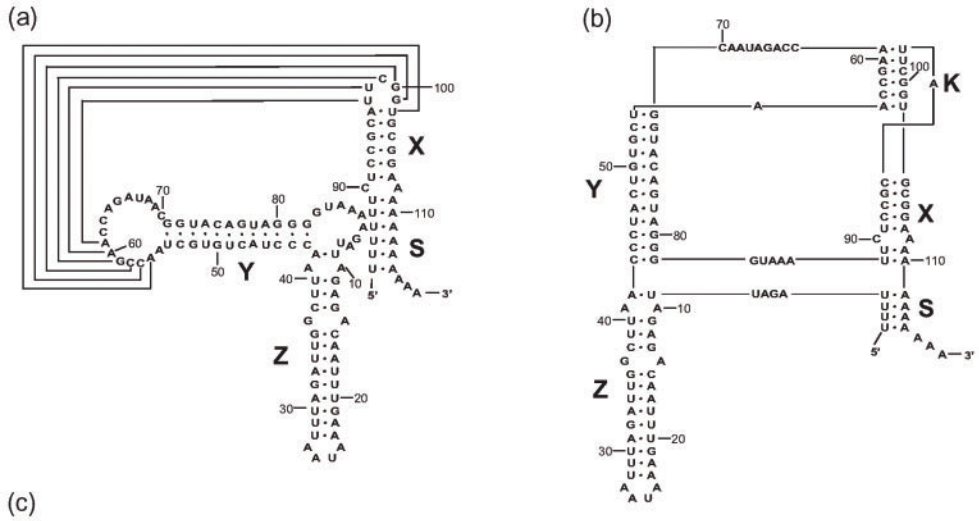

(d)

	Y	Y-K	K	K-Y	Y	Y-X	X	X-K	K	X
PV1	CCCUACCUCAGU		CGAAUU	GGAUUGGGUCAU	ACUGCUGUAGGG	GUAAA	UUUUUCUU	U	AAUUCG	GAGGAAAA
PV2	CCCUACCUCAGU		CGAAUU	GGAUUGGGUCAU	GCUGUUGUAGGG	GUAAA	UUUUUCUU	U	AAUUCG	GGGAAAAA
PV3S	CCCUACCUCAGU		CGAAUU	GGAUUGGGUCAU	ACUGUUGUAGGG	GUAAA	UUUUUCUU	U	AAUUCG	GAGGAAAA
CA21	CCCUACCUCAGU		CGGAUU	CGGAUUGGGUUAU	ACUGUUGUAGGG	GUAAA	UUUUUCUU	U	AAUUCG	GAGAAAAA
CA24	CCCUACCUCAGU		CGAAUU	GGAUUGGGUUAU	ACUGUUGUAGGG	GUAAA	UUUUUCUU	U	AAUUCG	GAAAAAAA
EV71	CCCCACCGGAA	A	UCUGGU	CGCGUUAAU	GACUGGUGGGG	GUAAA	UUUGUUAU	A	ACCAGA	AUAGCAAA
CA9	CCCUACUGUACU	A	ACCGAA	CUAGAUAAC	GGUGCAGUAGGG	GUAAA	UUCUCCGC	A	UUCGGU	GCGGAGGA
CA16	CCCCACCAGGG	A	UCUGGU	CGUGAAUAU	GACUGGUGGGG	GUAAA	UUUGUUAU	A	ACCAGA	AUAGCAAA
CB1	CCCUACCGCACU	A	ACCGAA	CUAGAUAAC	GGUGCAGUGGGG	GUAAA	UUCUCCGC	A	UUCGGU	GCGAAAAA
CB3A	CCCUACUGUGCU	A	ACCGAA	CCAGAUAAC	GGUACAGUAGGG	GUAAA	UUCUCCGC	A	UUCGGU	GCGGAAAA
CB4A	CCCUACUGCACU	A	ACCGAA	CUAGAUAAC	GGUGCAGUAGGG	GUAAA	UUCUCCGC	G	UUCGGU	GCGGAAAA
CB5	CCCUACCGCACC	A	ACCGAA	CUAGACAAC	GGUGCGGUAGGG	GUAAA	UUAUCCGC	A	UUCGGU	GCGGGAAA
ECHO6	CCCUACUGCACU	U	ACCGAA	CUAGAUAAU	GGUGUAGUAGGG	GUAAA	UUCUCCGC	A	UUCGGU	GCGGAAAA
ECHO9DM	CCCUACCGCACU	U	ACCGAA	CUAGACAAU	GGUGCGAUAGGG	GUAAA	UUCUCCGC	A	UUCGGU	GCGAAAAA
ECHO9BARTY	CCCUACCGCAUG	A	ACCGAA	CUUGAUACA	AGUGCGGUAGGG	GUAAA	UUCUCCGC	A	UUCGGU	GCGAAAAA
ECHO9HILL	CCUUACUGCACU	A	ACCGAA	CUAGAUAAC	GGUGCAGUAGGG	GUAAA	UUCUCCGC	A	UUCGGU	GCGAAAAA
ECHO11	CCCUACUGCACU	U	ACCGAA	CUAGAUAAC	GGUGUAGUAGGG	GUAAA	UUCUCCGC	A	UUCGGU	GCGAAAAA
ECHO12	CCCUACUGUACU	A	ACCGAA	CUAGACAAC	GGUGCAGUAGGG	GUAAA	UUCUCCGC	A	UUCGGU	GCGAAAAA

Fig. 1. Structure models of the coxsackievirus B3 *ori*R. (a) Secondary and (b) tertiary structure of the coxsackievirus B3 *ori*R. The *ori*R consists of three hairpin structures designated domains X, Y and Z. The structure can be closed by an interaction between the poly(A) and a 4 nt U stretch (S). The X domain can be stacked to the kissing (K) interaction to form one coaxial helical element connected by single-stranded nucleotide stretches ($GUAAA_{83–87}$, A_{55} and $CCAGAUAAC_{62–70}$) to a second coaxial helical domain, Z–Y. (c) Three-dimensional model of the closely related poliovirus *ori*R, obtained by molecular modelling (Pilipenko *et al*., 1996). The different specific domains are shown in different colours: K domain in white, K–Y linker $CCAGAUAAC_{62–70}$ in yellow, A_{55} bridging residue in light green, X domain in cyan, Y domain in orange, X–Y $GUAAA_{83–87}$ linker in red, AGAU sequence in green and S domain in purple. Fig. 1(c) can also be viewed as a rotating figure in JGV Online. (d) Comparative alignment for enteroviral *ori*R sequences. The domains are indicated in the figure.

The coxsackievirus B3 K and Y domains are linked by a single-stranded spacer of 9 nt (5′-CCAGAUAAC-3′, K–Y) and a single adenosine nucleotide spacer (Y–K) connecting the bottom of the K with the Y domain (Fig. 1a–d). Covariance analysis showed that the length and sequence of the spacers (K–Y and Y–K) are conserved in the human B enteroviruses (Fig. 1d). Although also conserved, the K–Y spacer is 12 nt in poliovirus-like enteroviruses, but lacks the single bridging nucleotide (Fig. 1d). To investigate the significance of the single-stranded linkers, a series of mutants was designed in which the spacers were either shortened or enlarged. Mutations were introduced into the pRibCB3/T7-cDNA clone (an infectious cDNA clone derived from the coxsackievirus B3 Nancy strain; van Ooij *et al.*, 2006), by PCR using forward primer 5′-ACTCTAC-GCTTTAAATGGTTGGACTCCTTTTAG-3′, containing a blunt *Dra*I restriction site (underlined), in combination with mutagenic oligonucleotides containing *Sal*I restriction sites (Table 1). PCR products were digested with *Dra*I and *Sal*I and subcloned in pRibCB3/T7-*Stu* digested with *Stu*I and *Sal*I. In the first two mutants, the spacer bridging the top of the K domain and the Y helix was shortened by 3 (Y_6, deleting $GAU_{65–67}$) or 6 (Y_3, deleting $GAUAAC_{65–70}$) nt. Another mutant was engineered in which the length of the spacer was increased by 3 nt (Y_{12}) by duplicating the CCA stretch, resulting in a mutant with a poliovirus-like spacer of 12 nt (5′-CCACCAGAUAAC-3′) (Fig. 1d). Also, a mutant was constructed in which the single adenosine (A_{55}) bridging the bottom Y helix to the K domain was deleted.

The effect of the mutations on the viral phenotype was tested by transfecting BGM cells with 4 μg RNA transcript derived from *Mlu*I-digested pRibCB3/T7 mutant plasmids. A cytopathic effect was observed for all mutants. Sequence analysis showed that all recovered viruses retained their engineered mutation. A plaque assay was used to determine the growth characteristics of the recovered viruses. Six-well dishes with a confluent monolayer of BGM cells were incubated with 10-fold serial dilutions of mutant or wild-type virus. After 30 min incubation at room temperature, cells were overlaid with 2·5 ml 1 × M199 containing 3 % fetal calf serum, 1 % glutamine, 0·5 % gentamicin, 0·5 % penicillin, 0·5 % Fungizone, 1 % $MgCl_2$ (2·5 M) and 1·3 % sodium bicarbonate (7·5 % solution) in 0·6 % agar (1 : 1 mixture of 1·2 % agar and 2 × M199). Cells were fixed by 2 ml methanol/acetic acid (3 : 1, v/v) at 48 h following infection, stained with 1 ml crystal violet (0·5 % crystal violet in 20 % ethanol) and destained by using tap water. Both mutant viruses containing a shortened single-stranded spacer exhibited a severe debilitating phenotype with small plaques at 36 °C. At 39 °C, minute plaques were observed for the $GAU_{65–67}$ deletion (Fig. 2a, Y_6), whereas the $GAUAAC_{65–70}$ deletion (Y_3) only showed plaques after extended incuation periods, indicative of a very severe defect in virus replication. In contrast, the poliovirus-like coxsackievirus mutants with the enlarged linker (Y_{12}) or the A_{55} deletion exhibited growth characteristics similar to those of wild-type coxsackievirus B3 at both 36 and 39 °C (Fig. 2a).

The bridging between the helical domains X and Y is formed by a single-stranded 5′-GUAAA-3′ spacer (Y–X). This Y–X linker is highly conserved among all human enteroviruses analysed to date (Fig. 1d). As we have described previously, analysis of mutants affecting the length of the helical domains X and Y allowed us to conclude that there are crosstalking events between the bottoms (probably the bottom $U_{88} \cdot A_{110}$ and $C_{43} \cdot G_{82}$ base pairs; Fig. 1) of the helices (Melchers *et al.*, 2000). In other words, these bottom base pairs should be recognized simultaneously and in a coordinated way. We have also shown that changes in the length of the helical elements do not bring about changes in the spatial position of, among others, the 5′-GUAAA-3′ spacer joining these two helical domains (Melchers *et al.*, 2000). To assess whether the length of the single-stranded spacer itself might contribute to phenotypical changes possibly associated with the orientation of the helical elements, mutants were designed in which the length of the 5′-GUAAA-3′ spacer, joining helical elements K–X and Y, was either deleted, shortened or enlarged (Fig. 2c). Following transfection, all designed mutations resulted in mutant viruses. Assessment of the replication kinetics of these mutant viruses at both 36 and 39 °C showed that a complete or partial deletion of the GUAAA spacer severely debilitated virus propagation at 36 °C (Fig. 2c). At 39 °C, minute plaques were only observed upon extended incubation periods for the complete GUAAA deletion and the GUA deletion mutant, whilst a small-plaque phenotype was observed for the GUAAA→GUAA mutant (Fig. 2c). Enlarging the Y–X spacer by an additional three residues (GUAAA to GUAAAAAA) resulted in a mutant virus that was severely temperature-sensitive, as evidenced by the pinprick plaques at 39 °C, but close to wild-type growth characteristics at 36 °C (Fig. 2c). Therefore, both increasing and decreasing the length of this spacer affected virus replication, possibly resulting from a disorientation of the bottom base pairs as described previously (Melchers *et al.*, 2000), and thereby an altered geometry of the overall structure (Fig. 1c).

There are only limited data available on the functional aspects of interconnecting single-stranded regions, but the J/J5a linker that joins the two halves of the P4–P6 domain of the *Tetrahymena* self-splicing group I intron acts as a hinge, allowing the coaxially stacked elements on either side of it to interact via specific tertiary contacts (Szewczak & Cech, 1997). Indeed, shortening the coxsackievirus *ori*R Y–X and K–Y linkers resulted in highly disabled mutant viruses. Again, this may be the result of disturbed ligand binding. On the other hand, phenotypic effects of the local rotation of one or more base pairs in either domain X or domain Y suggested that the two distal base pairs of these domains serve as orientation-dependent recognizable signals (Melchers *et al.*, 2000). Shortening the proximal spacer may increase the pressure on the distance

Table 1. Oligonucleotides used for mutagenesis by PCR and the Altered Sites *in vitro* mutagenesis system (Promega)

Italics represent the *Sal*I restriction site; introduced mutations are underlined.

Mutant	Sequence PCR oligonucleotide (5′→3′ orientation)
ΔGUAAA	GGGGGGGG*GTCGAC*ACGCGT$_{28}$CCGCACCGAATGCGGAGAACCCTACTGTACCGTTATC
GUAAA→AA	GGGGGGGG*GTCGAC*ACGCGT$_{28}$CCGCACCGAATGCGGAGAATTCCCTACTGTACCGTTATC
GUAAA→AAAAA	GGGGGGGG*GTCGAC*ACGCGT$_{28}$CCGCACCGAATGCGGAGAATTTTTCCCTACTGTACCGTTATC
GUAAA→GUA$_6$	GGGGGGGG*GTCGAC*ACGCGT$_{28}$CCGCACCGAATGCGGAGAATTTTTTACCCCTACTGTACCGTTATC
GUAAA→GAAAA	GGGGGGGG*GTCGAC*ACGCGT$_{28}$CCGCACCGAATGCGGAGAATTT*T*CCCCTACTGTACCGTTATC
GUAAA→AUAAA	GGGGGGGG*GTCGAC*ACGCGT$_{28}$CCGCACCGAATGCGGAGAATTTATCCCTACTGTACCGTTATC
GUAAA→GUAA	GGGGGGGG*GTCGAC*ACGCGT$_{28}$CCGCACCGCATGCGGAGAATTACCCCTACTGTACCGTTATC
GUAAA→GUAAC	GGGGGGGG*GTCGAC*ACGCGT$_{28}$CCGCACCGAATGCGGAGAAGTTACCCCTACTGTACCGTTATC
GUAAA→GUAUA	GGGGGGGG*GTCGAC*ACGCGT$_{28}$CCGCACCGAATGCGGAGAATATACCCCTACTGTACCGTTATC
$_{7355}$CCAGAUAAC$_{7363}$→CCAAAC Y$_9$→Y$_6$	GGGGGGGGG*GTCGAC*ACGCGT$_{28}$CCGCACCGAATGCGGAGAATTTACCCCTACTGTACCGTTTGGTTCGGTTAGCACAG
$_{7355}$CCAGAUAAC$_{7363}$→CCA Y$_9$→Y$_3$	GGGGGGGG*GTCGAC*ACGCGT$_{28}$CCGCACCGAATGCGGAGAATTTACCCCTACTGTACCTGGTTCGGTTAGCACAGTAGG-GTTAAG
$_{7355}$CCAGAUAAC$_{7363}$→CCACCAGAUAAC Y$_9$→Y$_{12}$	GGGGGGGG*GTCGAC*ACGCGT$_{28}$CCGCACCGAATGCGGAGAATTTACCCCTACTGTACCGTTATCTGGTGGTTCGGTTAG-CACAGTAGGGTTAAG
U$_{7360}$A	GGGGGGGG*GTCGAC*ACGCGT$_{28}$CCGCACCGAATGCGGAGAATTTACCCCTACTGTACCGTTTTCTGGTTCGGTTAGCAC
A$_{7362}$C	GGGGGGGG*GTCGAC*ACGCGT$_{28}$CCGCACCGAATGCGGAGAATTTACCCCTACTGTACCGGTATCTGGTTCGGTTAGCAC
C$_{7363}$G	GGGGGGGG*GTCGAC*ACGCGT$_{28}$CCGCACCGAATGCGGACAATTTACCCCTACTGTACCCTTATCTGGTTCGGTTAGCAC
	Altered Sites mutant oligonucleotide (5′→3′ orientation)
C$_{7355}$G	GTACCGTTATCTGCTTCGGTTAGCACAG
C$_{7356}$G	TGTACCGTTATCTCGTTCGGTTAGCACAG
A$_{7357}$U	CTGTACCGTTATCAGGTTCGGTTAGCACAG
G$_{7358}$C	ACTGTACCGTTATGTGGTTCGGTTAGCAC
A$_{7359}$C	TACTGTACCGTTAGCTGGTTCGGTTAGCAC
A$_{7361}$U	CCTACTGTACCGTAATCTGGTTCGGTTAG

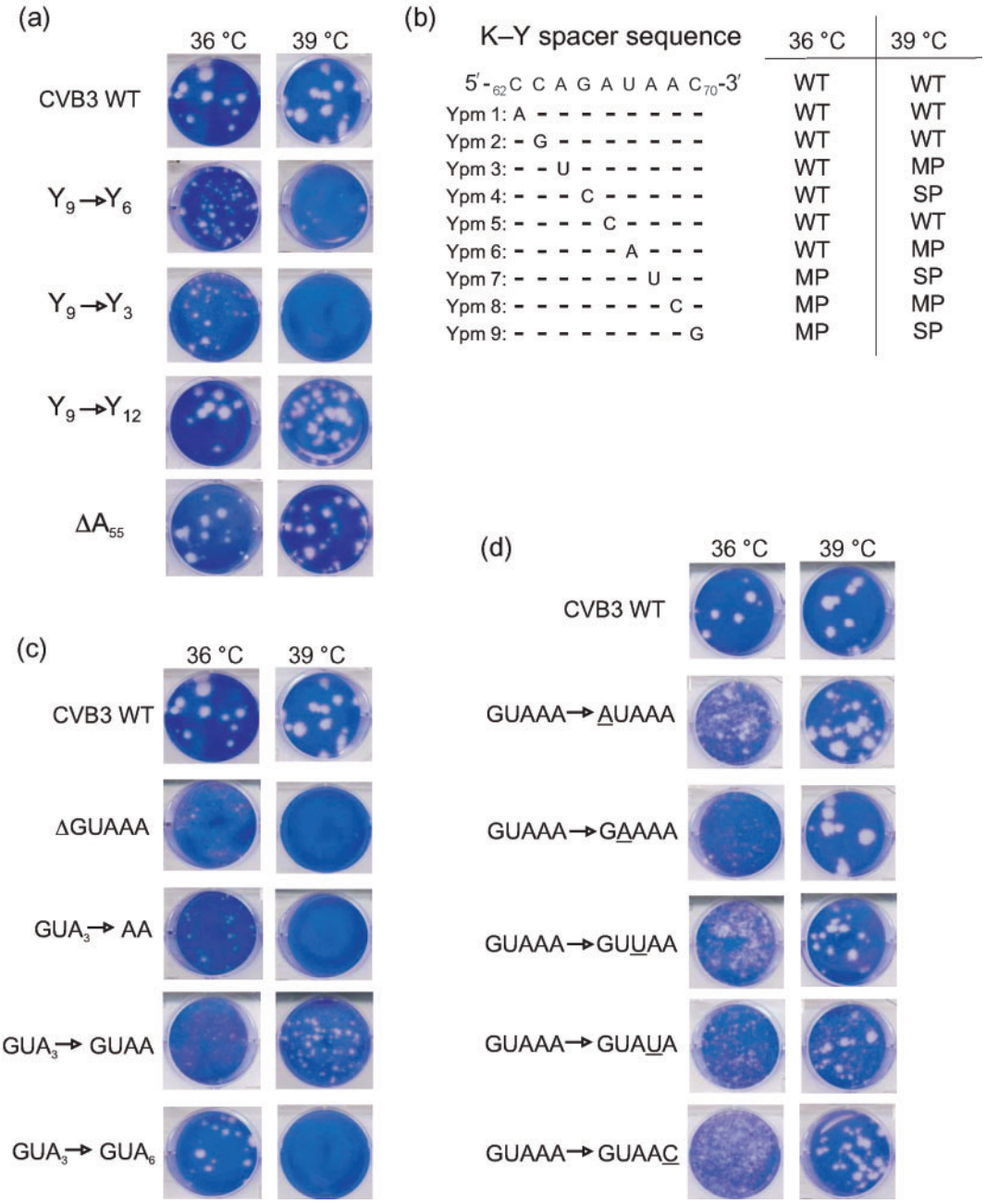

Fig. 2. (a) Plaque phenotypes are depicted of the wild-type virus and the K–Y linker mutants at 36 and 39 °C. (b) Results of the plaque assays for the K–Y linker CCAGAUAAC$_{62-70}$ point mutants at 36 and 39 °C. WT, Wild-type plaque phenotype; MP, medium-plaque phenotype; SP, small-plaque phenotype. (c, d) Plaque phenotypes of the wild-type virus and the X–Y GUAAA$_{83-87}$ linker-length mutants (c) and the plaque assays for the X–Y linker point mutants at 36 and 39 °C (d). The mutations are underlined. CBV3, Coxsackievirus B3. For further details, see text.

and orientation of the distal base pairs, as in the ends of a clothes peg. Increasing the length, on the other hand, may increase the flexibility of the loop, which can be anticipated by the coaxial helical domains without affecting the overall geometry of the molecule. Indeed, this mutant did not manifest itself in phenotypic alterations at 36 °C (Fig. 2c).

To investigate the physiological importance of the primary sequence, a point-mutational analysis was undertaken in which each base of the K–Y and Y–X single-stranded spacers was mutated individually without affecting the overall secondary structure of the *ori*R (as determined by Mfold computer predictions; Zuker *et al.*, 1999). The specific mutations are shown in Fig. 2(b, d). All mutated

coxsackievirus B3 full-length transcripts rendered virus upon transfection. The mutant K–Y viruses could be grouped into three classes depending on their growth properties (Fig. 2b). In one group, the mutations did not result in a phenotypic alteration. This group consisted of the 5′ mutations directly flanking the kissing interaction (i.e. Ypm1, Ypm2 and Ypm3) and mutant virus Ypm5, containing a mutation localized in the middle portion of the K–Y spacer. In the second group, mutant viruses Ypm4 and Ypm6 also had wild-type growth characteristics at 36 °C, but appeared to be thermosensitive (Fig. 2b). The last group, mutant virus Ypm7, Ypm8 and Ypm9, containing mutations flanking the Y-helical domain, were all severely affected in growth at both 36 and 39 °C (Fig. 2b). The negative effect on replication of a number of point mutations (especially those flanking the Y domain) may reflect the disturbance of a necessary local geometry. On the other hand, these mutations may disturb specific interactions with replication proteins that depend on such sequence-based recognition (Harris *et al.*, 1994; Mellits *et al.*, 1998; Todd *et al.*, 1995; Waggoner & Sarnow, 1998). Of all the Y–X spacer point mutations introduced, only the AUAAA mutant was found to revert back to wild-type *ori*R sequence in two out of the three transfections performed, whereas all others had retained the engineered substitution after transfection. Interestingly, although each point mutation altering the sequence resulted in defective growth characteristics at 36 °C, the mutations did not manifest a phenotypic alteration at 39 °C, indicating a cold-sensitive mutant (Fig. 2d). The observation of wild-type growth characteristics at higher temperatures suggests that the 5′-GUAAA-3′ spacer may adopt a specific structure. Although this observation is difficult to explain, this structure might be affected by the specific point mutations at the optimal temperature (36–37 °C), resulting in an adverse effect on replication due to the destabilization of recognition signals. At higher temperatures, these point mutations might be tolerated because of increased movement of the molecule, thereby compensating the effect on replication. A complete deletion of this GUAAA spacer in poliovirus has been shown to abolish RNA replication at the level of negative-strand RNA synthesis by using a cell-free replication system (Barton *et al.*, 2001; Morasco *et al.*, 2003). Although ultimately this mutation does give rise to (highly debilitated) viruses, from these results it can be concluded that the GUAAA sequence is of importance for an efficient initiation of RNA synthesis.

In conclusion, our results show the importance of the single-stranded regions linking the two coaxially stacked helices K–X–S and Y–Z in the coxsackievirus *ori*R and demonstrate that the intrinsic connection between *ori*R structure and function is fine-tuned by the spacing between these coaxial RNA helices. Obviously we are aware of the limitations to understand large RNA structures by studying the effects of altering structural domains using biochemical/virological approaches. However, as long as large, complex RNA molecules elude high-resolution structure determination by nuclear magnetic resonance or X-ray crystallography, virological/biochemical experiments are important to elucidate the structure–function relationship of RNA elements.

Acknowledgements

This research was supported by the Netherlands Organization for Scientific Research, Chemical Council (NWO-CW 98008).

References

Agol, V. I., Paul, A. V. & Wimmer, E. (1999). Paradoxes of the replication of picornaviral genomes. *Virus Res* **62**, 129–147.

Andino, R., Rieckhof, G. E. & Baltimore, D. (1990). A functional ribonucleoprotein complex forms around the 5′ end of poliovirus RNA. *Cell* **63**, 369–380.

Barton, D. J., O'Donnell, B. J. & Flanegan, J. B. (2001). 5′ cloverleaf in poliovirus RNA is a *cis*-acting replication element required for negative-strand synthesis. *EMBO J* **20**, 1439–1448.

Gamarnik, A. V. & Andino, R. (1998). Switch from translation to RNA replication in a positive-stranded RNA virus. *Genes Dev* **12**, 2293–2304.

Gamarnik, A. V. & Andino, R. (2000). Interactions of viral protein 3CD and poly(rC) binding protein with the 5′ untranslated region of the poliovirus genome. *J Virol* **74**, 2219–2226.

Harris, K. S., Xiang, W., Alexander, L., Lane, W. S., Paul, A. V. & Wimmer, E. (1994). Interaction of poliovirus polypeptide $3CD^{pro}$ with the 5′ and 3′ termini of the poliovirus genome. *J Biol Chem* **269**, 27004–27014.

Herold, J. & Andino, R. (2001). Poliovirus RNA replication requires genome circularization through a protein–protein bridge. *Mol Cell* **7**, 581–591.

Melchers, W. J. G., Hoenderop, J. G. J., Bruins Slot, H. J., Pleij, C. W. A., Pilipenko, E. V., Agol, V. I. & Galama, J. M. D. (1997). Kissing of the two predominant hairpin loops in the coxsackie B virus 3′ untranslated region is the essential structural feature of the origin of replication required for negative-strand RNA synthesis. *J Virol* **71**, 686–696.

Melchers, W. J. G., Bakkers, J. M. J. E., Bruins Slot, H. J., Galama, J. M. D., Agol, V. I. & Pilipenko, E. V. (2000). Cross-talk between orientation-dependent recognition determinants of a complex control RNA element, the enterovirus *ori*R. *RNA* **6**, 976–987.

Mellits, K. H., Meredith, J. M., Rohll, J. B., Evans, D. J. & Almond, J. W. (1998). Binding of a cellular factor to the 3′ untranslated region of the RNA genomes of entero- and rhinoviruses plays a role in virus replication. *J Gen Virol* **79**, 1715–1723.

Mirmomeni, M. H., Hughes, P. J. & Stanway, G. (1997). An RNA tertiary structure in the 3′ untranslated region of enteroviruses is necessary for efficient replication. *J Virol* **71**, 2363–2370.

Morasco, B. J., Sharma, N., Parilla, J. & Flanegan, J. B. (2003). Poliovirus *cre*(2C)-dependent synthesis of VPgpUpU is required for positive- but not negative-strand RNA synthesis. *J Virol* **77**, 5136–5144.

Parsley, T. B., Towner, J. S., Blyn, L. B., Ehrenfeld, E. & Semler, B. L. (1997). Poly (rC) binding protein 2 forms a ternary complex with the 5′-terminal sequences of poliovirus RNA and the viral 3CD proteinase. *RNA* **3**, 1124–1134.

Pilipenko, E. V., Poperechny, K., Maslova, S. V., Melchers, W. J. G., Bruins Slot, H. J. & Agol, V. I. (1996). *Cis*-element, *ori*R, involved in the initiation of (−) strand poliovirus RNA: a quasi-globular

multi-domain RNA structure maintained by tertiary ('kissing') interactions. *EMBO J* **15**, 5428–5436.

Szewczak, A. A. & Cech, T. R. (1997). An RNA internal loop acts as a hinge to facilitate ribozyme folding and catalysis. *RNA* **3**, 838–849.

Todd, S., Nguyen, J. H. & Semler, B. L. (1995). RNA-protein interactions directed by the 3′ end of human rhinovirus genomic RNA. *J Virol* **69**, 3605–3614.

van Ooij, M. J. M., Vogt, D. A., Paul, A. & 7 other authors (2006). Structural and functional characterization of the coxsackievirus B3 CRE(2C): role of CRE(2C) in negative- and positive-strand RNA synthesis. *J Gen Virol* **87**, 103–113.

Waggoner, S. & Sarnow, P. (1998). Viral ribonucleoprotein complex formation and nucleolar-cytoplasmic relocalization of nucleolin in poliovirus-infected cells. *J Virol* **72**, 6699–6709.

Wang, J., Bakkers, J. M. J. E., Galama, J. M. D., Bruins Slot, H. J., Pilipenko, E. V., Agol, V. I. & Melchers, W. J. G. (1999). Structural requirements of the higher order RNA kissing element in the enteroviral 3′UTR. *Nucleic Acids Res* **27**, 485–490.

Zuker, M., Mathews, D. H. & Turner, D. H. (1999). Algorithms and thermodynamics for RNA secondary structure prediction: a practical guide. In *RNA Biochemistry and Biotechnology*, pp. 11–43. Edited by J. Barciszewski & B. F. C. Clark. Dordrecht, The Netherlands: Kluwer Academic Publishers.